

# A CHANNEL OF HIGH CURRENT DEUTERON LINAC WITH LOW RADIATION LOSSES

**P.O. Demchenko, Ye.V. Gussev, M.G. Shulika**

*National Science Center "Kharkov Institute of Physics and Technology", Kharkov, Ukraine*  
e-mail: [demchenko@kipt.kharkov.ua](mailto:demchenko@kipt.kharkov.ua)

The performances of an accelerating channel of a high-current deuteron linac for production of  $^{99}\text{Mo}$ - $^{99m}\text{Tc}$  medical radioisotope-generator are given. The radioisotope is produced by deuteron beam bombardment of natural molybdenum targets. The mean yield of  $^{99}\text{Mo}$  radioisotope is no less than 0.16 Ci/h. The produced radioisotope has the high radionuclide purity. The accelerating channel has been calculated for average beam current of 1 mA, and deuteron energy of 14 MeV. The longitudinal and transverse movement stabilities of charged particle beam are ensured with *RF* accelerating electric field. The initial section is the radio frequency quadrupole with the output energy of 2 MeV, and two other sections are structures with modified alternative-phase focusing. Low deuteron losses in the accelerating channel result in low induced activity of accelerating structure elements.

PACS: 29.17.+W, 29.27.-A, 47.75.AK

## 1. INTRODUCTION

The short-lived radioisotopes are widely used in medicine for diagnostics both pathological structural changes of internal organs and functional disorders of patient vital systems. About 90 % radionuclide diagnostics examinations are done using technetium-99m with half-life of 6 h. Its extensive application is due to a low energy of emitted  $\gamma$ -rays (141 keV), and other physical and chemical properties permitting to use this radioisotope as a radioactive tracer for many pharmaceuticals used in medical diagnostics [1].

In the nature there is no  $^{99m}\text{Tc}$ . Technetium-99m is a daughter product of molybdenum - 99  $\beta^-$ -decay with 66 hours half-life. Now  $^{99}\text{Mo}$  is chemically evolved from high radioactive fission products of uranium - 235. Before that high-enriched  $^{235}\text{U}$  targets are irradiated by neutrons in a nuclear reactor. As nuclear reactors are potentially dangerous objects because of possible accidents due to runaway, and the uranium-235 is a fissile material that can be used for illegal nuclear arms production, therefore alternative methods are being searched for  $^{99}\text{Mo}$ - $^{99m}\text{Tc}$  radioisotope-generator production [1,3,5,6].

To avoid uncontrolled nuclear reactor runaway is possible if it operates in a subcritical mode. In this case an external neutron source is needed for reactor driving [2]. In particular, for ADONIS project a proton cyclotron with particle energy of 150 MeV and beam current of 2 mA is supposed to use for subcritical reactor control [2]. However, in this case there is a danger of fissile uranium-235 proliferation.

To exclude completely problems of reactor  $^{99}\text{Mo}$  production electron or ion accelerators may be used [1,3,5,6].

Accelerated electrons do not take part directly in nuclear reactions with transmutation of chemical element isotopes. Preliminarily electron beam energy is converted to  $\gamma$ -radiation. For that accelerated electrons are retarded in a heavy metal target [1,5]. If the  $\gamma$ -ray energy is higher than photonuclear reaction threshold, a nucle-

on detachment from nucleus is observed, i.e. reactions of  $(\gamma, n)$ ,  $(\gamma, 2n)$ ,  $(\gamma, p)$ , etc.

For production  $^{99}\text{Mo}$  on electron accelerators the capture of photoneutrons by  $^{98}\text{Mo}$  isotope can be used, i.e.  $^{98}\text{Mo}(n, \gamma)^{99}\text{Mo}$  reaction, or a photodetachment of a neutron from  $^{100}\text{Mo}$  isotope, i.e. the reaction of  $^{100}\text{Mo}(\gamma, n)^{99}\text{Mo}$ . The later reaction is more effective [1]. The  $\gamma$ -rays have a long path in a metal molybdenum target that is why the specific activity of the obtained radionuclide is low. The  $^{99}\text{Mo}$  yield can be increased if enriched (~96 %) molybdenum-100 isotope targets are used. The specific cost of such targets is high enough ~1000 \$/g, and the weight of required target is about 14g [1].

Accelerated ions during collisions in the target interact directly with nuclei resulting in isotope transmutation and new particle production. In this case the different channels of reactions are simultaneously possible dependently on both the ion energy and particle kind and a target nucleus [3,4].

The analysis shows that taking into account the cost of target materials, radionuclide separation technology and power consumption the optimal  $^{99}\text{Mo}$  radioisotope production may be obtained if accelerated deuteron beams with the energy of 12...15 MeV and the thin natural molybdenum targets are used [6].

In section 2 of the paper the physics and technology requirements to a deuteron accelerator for producing of the  $^{99}\text{Mo}$ - $^{99m}\text{Tc}$  radioisotope-generator in practical amount are given. In addition, it is argued the application of a high current deuteron linac in which accelerating and focusing of a beam are done by the same *RF* electric field. In section 3 the results of numerical simulation of deuteron beam dynamics in the initial part of the accelerating channel are presented. The initial part is a section with radio frequency quadrupole focusing (*RFQ*) [10]. Results of numerical simulation of deuteron beam dynamics in the next sections based on modified alternating-phase focusing (*MAPF*) [7] are given in section 4. Here some questions of matching of beam performances between sections are also considered.

In the process of computation and optimization of the accelerating channel the considerable attention had been given to minimization of deuteron losses on accelerating structures elements, i.e. to the accelerator radiation purity.

## 2. REQUIREMENTS TO A DEUTERON ACCELERATOR

The activity  $A_i(t)$  of produced  $i$ -kind rationuclide depending on target irradiation time  $t$  by an ion beam with the current of  $I_b$  is determined by the expression:

$$A_i(t) = (p_i I_b / e) \left( 1 - e^{-0.693t/\tau_{1/2}} \right), \quad (1)$$

where  $\tau_{1/2}$  is the period of radioisotope half decay,  $e$  is the ion charge, and probability  $p_i$  of  $i$ -radionuclide producing in collisions with  $j$ -nuclides of target is

$$p_i = \sum_j \int_0^{R(W_0)} \sigma_{ij}(W) N_j dx. \quad (2)$$

Here  $\sigma_{ij}(W)$  is the dependence of corresponding nuclear reaction cross-section on the energy  $W$  of bombarding particles,  $N_j$  is the  $j$ -kind nucleus density in the target,  $x(W)$  is the target length that the particle penetrates retarding from the initial energy  $W_0$  to  $W$  energy,  $R(W_0)$  is the path length of bombarding particles in the target. Summing in (2) is carried out over all  $j$ -nuclides of target the reactions with that give  $i$ -rationuclide.

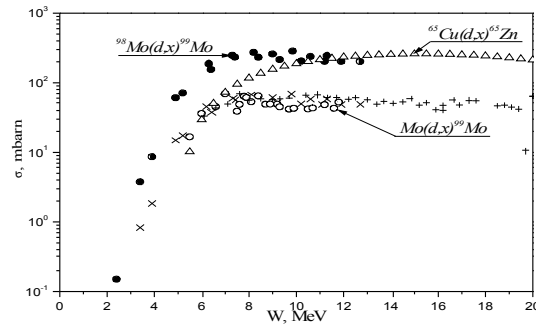
Since the rationuclide decay occurs simultaneously with its production then according to (1) the equilibrium activity  $A_\infty$  is attained if irradiation time is  $t > 2\tau_{1/2}$  (for  $t=2\tau_{1/2}$ ,  $A_i(t) \approx 0.75A_\infty$ ). If exposition duration  $t$  is  $t < \tau_{1/2}$  then the activity of the obtained radio-nuclide is  $A_i \sim t$ .

From (1) and (2) it follows that to decrease capital expanses for accelerator building and the cost of electrical power supply the ion kind and also the target isotope composition have to be chosen such a way to have the maximum cross-sections of corresponding nuclear reactions at the minimum bombarding particles energy of  $W_0$ . Besides, for relatively low energies the number of allowed nuclear reaction channels are limited that permits to obtain the sufficient rationuclide purity of the desired radioisotope without subsequent chemical treatment.

The analysis of experimental data on ion nuclear reaction cross-sections that produce the  $^{99}\text{Mo}$  isotope shows that an accelerated deuteron beam and a target from the natural molybdenum either enriched by  $^{98}\text{Mo}$  or  $^{100}\text{Mo}$  is the most optimal choice. The contents of  $^{98}\text{Mo}$  and  $^{100}\text{Mo}$  in the natural target are 23.78 %, and 9.63 % respectively.

Dependences on energy of  $^{99}\text{Mo}$  production cross-sections on targets from the natural molybdenum and  $^{98}\text{Mo}$  are shown in Fig. 1 [4,11]. At low deuteron energies the reaction of  $^{98}\text{Mo}(d,p)^{99}\text{Mo}$  dominates with the threshold  $Q=3.7$  MeV. The maximum cross-section of this reaction is about 240 mbarn for  $W \approx 11$  MeV, Fig. 1. With the energy growth the additional channels of  $^{100}\text{Mo}(d,dn)^{99}\text{Mo}$  ( $Q=8.9$  MeV) and  $^{100}\text{Mo}(d,p2n)^{99}\text{Mo}$  ( $Q=10.5$  MeV) on the  $^{100}\text{Mo}$  isotope are opened [4]. As a result the total cross-section to produce of  $^{99}\text{Mo}$  isotope on a natural molybdenum target is the approximately

constant of  $\sigma \approx 60$  mbarn for the wide deuteron energy range of  $7 \leq W \leq 21$  MeV, Fig. 1. At the deuteron energy of  $W < 15$  MeV the amount of contaminating long-lived radioisotopes of  $\text{Zr}$ ,  $\text{Nb}$ ,  $\text{Mo}$ ,  $\text{Tc}$  are negligible that permits to use the irradiated targets directly for preparation of  $^{99}\text{Mo}-^{99m}\text{Tc}$  radioisotope-generator [4].



mined with the duty factor of *RF* power supply. In linacs an average current may be reached dozens of milliamperes that is determined by *RF* power source availability and corresponding cooling of accelerator components. Therefore now the superconducting accelerating structures are being intensively investigated to decrease the power consumption considerably [12].

For any type of a deuteron accelerator there is a hard limit for particle losses resulting in induced activity of construction elements when the energy  $W$  is higher than the deuteron binding energy  $E_b=2.2$  MeV. For analysis of exposition doze field near a linac its channel can be presented as a set of copper cylindrical tubes. A basic contribution to induced activity, when deuteron energy is  $W \leq 14$  MeV, is made by nuclear reactions  $^{63}\text{Cu}(d,x)^{63}\text{Zn}$ ,  $^{65}\text{Cu}(d,x)^{65}\text{Zn}$ , cross-sections of which have maximum near  $W=14$  MeV, Fig. 1 [9]. Contents of  $^{63}\text{Cu}$  and  $^{65}\text{Cu}$  isotopes in copper are 69.09% and 30.9%, respectively [8]. Deuteron reactions with copper isotopes produce  $^{63}\text{Zn}$  and  $^{65}\text{Zn}$  radionuclides with half-lives of 38 min and 222 days respectively. The induced activity caused by the  $^{63}\text{Zn}$  rationuclide decreases rapidly when the accelerator is stopped. The  $^{65}\text{Zn}$  equilibrium activity will be reached after several years of accelerator run (1), and it remains approximately constant after the accelerator stop.

The estimations have shown that the acceptable linear particle losses at the end of the accelerating channel, i.e. at maximum deuteron energy, have to be no more than  $2 \cdot 10^{-8}$  A/m.

Design and construction parameters of a linac depend on many factors, in particular, on an injected ion energy  $W_i$ , a beam current amplitude  $I_0$ , a duty factor  $F_d$ , an operating frequency  $f$  of electric field, a type of accelerating structures, and the method of achievement of beam movement stability that determines the beam radiation losses in a channel. Important requirements to a technological accelerator are also a high operating reliability for a long time, minimum number of elements, which are needed in periodic adjustment, and so few power sources as possible.

Taking into account above requirements the linac channel had been calculated for injected deuteron energy of  $W_i=100$  keV [13], output energy of  $W_o=14$  MeV, current amplitude  $I_0=50$  mA, duty factor  $F_d=0.02$  (the average current  $I_b=1$  mA), operating frequency  $f=152.5$  MHz. Fig. 2, shows a layout of the accelerating channel without an injector, output devices, and a target unit. The feature of the accelerating channel (Fig 2) is that longitudinal and transverse beam movement stabilities are ensured by the same *RF* electric field. The bunching of injected beam and its preliminary accelerating up to  $W_i=2$  MeV are realized in the initial section with spatially uniform quadrupole focusing (*RFQ*) [10]. The main acceleration takes place in two sections (*MAPF-1*, *MAPF-2*) with modified alternating phase focusing [7], which output energies are 6.4 MeV and 14 MeV, respectively, Fig 2. Static electromagnetic quadrupole triplets  $T1-T4$  are used to match phase-space beam performances after passing the drifts between the accelerating sections.

A low level of induced activity had been reached due to that the main particle losses were localized in *RFQ* section, output energy of which was chosen  $W_i=2$  MeV, i.e. lower than the deuteron binding energy. Performances of the next accelerating sections have been calculated in such a way that particle losses in them did not exceed the allowed limits.

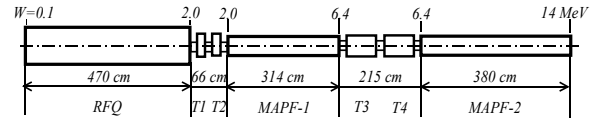


**Fig. 2. Accelerating channel:** *RFQ* is the section with radio-frequency quadrupole, *MAPF-1* and *MAPF-2* are sections with modified alternating-phase focusing,  $T1-T4$  are magnetic quadrupole triplets

Results of numerical simulation of high current deuterium beam dynamics in sections with different symmetry of *RF* accelerating and focusing fields are given below.

### 3. RADIO FREQUENCY QUADRUPOLE

As the initial part of modern high current ion accelerators are used *RFQ* structures [12]. *RFQ* has some important advantages: a respectively low injected ion energy, hard alternating-sign focusing by *RF* electrical field that is useful for bunching of low energy particle beams with a high space charge, a high beam transmission. The main disadvantages are a low accelerating rate, comparatively low shunt impedance that reduces power efficiency of accelerator when the ion energy is increased. Therefore after bunching and preliminary accelerating of ions to the energy of  $W_i=2\dots 6$  MeV/nucleon more effective structures are used instead of *RFQ*.

In this paper the Fourier-Bessel method had been used for numerical simulation of *RFQ* electrical field. The field of beam space charge had been taken into account by the particle-in-cell method. The assembly of  $10^3$  macroparticles was used for dynamics simulation, and it was increased up to  $10^4$  for particle losses calculation in the channel.

The computed *RFQ* section with the injected deuteron energy of 100 KeV and output energy of 2 MeV represents the modulated in the longitudinal direction four-transmission line with the voltage on adjacent electrodes  $U_0=78$  kV. In the transverse  $xy$  plane the electrodes form the electric field of quadrupole symmetry, the  $E_x$  and  $E_y$  components of which ensure the beam focusing. The longitudinal  $E_z$  field component, which is bunching and accelerating the beam, is produced by modulation of electrode distances from  $z$ -axes. The average distance is 5 mm, and the maximum electrical field on the electrodes surfaces reaches 226 kV/cm. The longitudinal electrode modulation profile is a trapeze, the length of which (an accelerating period) equals  $\beta\lambda/2$  and increases monotonously with increasing of the reduced ion velocity  $\beta=v/c$  ( $v$  is the ion velocity,  $c$  is the light velocity,  $\lambda$  is a wave length of the *RF* field).

The total number of accelerating periods is  $n=175$ . The electrode modulation ratio, i.e. the ratio of the ma-

ximum electrode distance from the system axis to minimum one, increases along the section from 1 to 1.56.

A high injected beam transmission factor can be obtained by adiabatic increasing of electric field component  $E_z$  along a channel, changing electrode modulation ratio. Simultaneously when the beam is being bunched the synchronous particle phase  $\varphi_s$ , the initial value of which is chosen of  $90^\circ$ , has to be slowly increased to give the growth of the acceleration rate [10,15].

Fig. 3 shows the synchronous phase distribution along the *RFQ* accelerating periods. As it follows from Fig. 3 the monotonous changing of  $\varphi_s$  is disturbed in 6, 7, 14, 19, 24 and 28 periods. It was caused that the  $E_z$  electric field was taken relatively high of  $E_z=4.9$  kV/cm for increasing of acceleration rate. At this field the strong longitudinal compression of bunches occurs in some initial periods. As a result the space charge density in the bunches was essentially increased that caused the fast beam expansion in the transverse plane  $xy$ . As a result high particle losses on accelerating channel elements occurred. To preserve the acceleration rate and decrease the losses the negative synchronous phases  $\varphi_s$  were altered to positive ones by increasing of the length of some periods, Fig. 3. The altering of  $\varphi_s$  sign reduces the longitudinal bunch compression in several initial periods and simultaneously increases hardness of transverse beam focusing. These effects are proportional to  $\sin\varphi_s$ . In this case the acceleration rate  $\Delta W/\Delta z \sim \cos\varphi_s$  does not change.

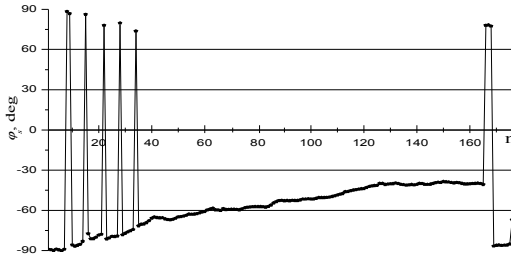


**Fig. 3.** Dependence of a synchronous phase  $\varphi_s$  on an accelerating period number  $n$  in the *RFQ*-section

As a result of using of the considered combination of alternating-phase and radio frequency quadrupole focusing the total beam transmission factor was reached 86.3 % for injected beam current 60 mA, and beam energy spread 0.25 % and normalized emittance  $\varepsilon_n \approx 0.1 \pi$  mm·mrad. For the beam matching to *RFQ* acceptance the injected beam must be convergent with envelope slope to the channel axis of 37.5 mrad. At the *RFQ* output the beam current was  $I_f=51.8$  mA and the deuteron energy  $W_f=2$  MeV.

The monotonous behavior of  $\varphi_s$  is also disrupted at the end of the *RFQ* section, Fig. 3. It is caused by the matching of phase space performances of preliminary *RFQ* accelerated deuteron beam to input parameters of the next *MAPF-1* section with alternating-phase focusing, Fig. 2. The section is located in the separate vacu-

um chamber and bounded with the *RFQ* section by a drift of 66 cm length.

As the *RFQ* section has quadrupole symmetric electric field and *MAPF-1* has axial symmetry of the field therefore it is necessary to match the beam parameters in three cross-sections of the phase space: ( $xx'$ ) and ( $yy'$ ) for two transverse components of beam movement and ( $\Delta\beta\Delta\varphi$ ) of the longitudinal one ( $\Delta\beta=\beta-\beta_s$ ,  $\beta_s=v/c$  is a reduced velocity of a synchronous particle,  $\Delta\varphi=\varphi_s-\varphi$ , where  $\varphi$  is a phase of a particle). The quality of matching has decisive importance for the particle losses in the next accelerator sections.

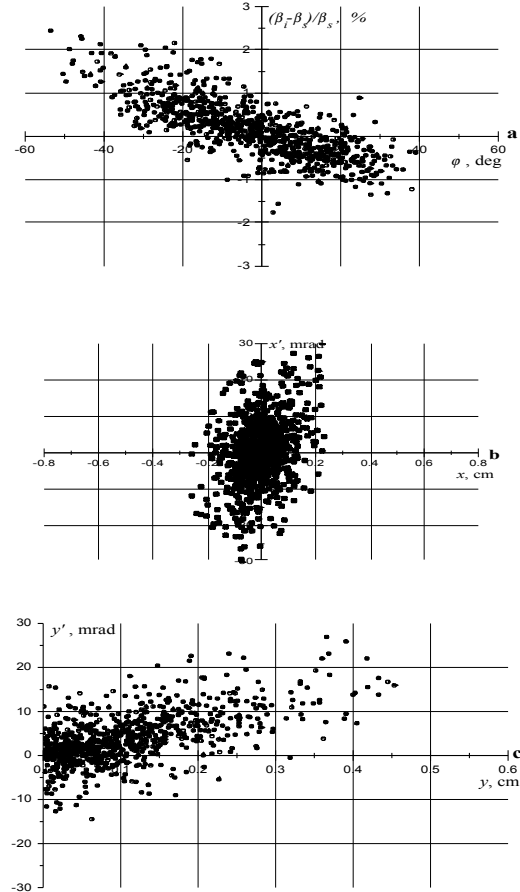


**Fig. 4.** Beam phase space plots at the *RFQ* output: a is longitudinal plane projection, b is  $xx'$  plane projection, c is  $yy'$  plane projection

For the longitudinal movement matching the synchronous phase values in the last accelerating periods of *RFQ* section have been chosen  $\varphi_s \approx -90^\circ$ , Fig. 3. It results in formation of convergent bunches in longitudinal direction at the section output, Fig. 4a. When the beam is passing along the drift the longitudinal crossover is formed initially and then bunches are converging. However at the *MAPF-1* input the phase extension of bunches  $\Delta\varphi_l$  is in limits of this section separatrix. Such matching is reached by the corresponding choice of the drift length between sections.

At the *RFQ* section output the bunches are divergent in the transverse movement plane  $xy$ , Fig. 4b and 4c.

Therefore for the beam matching to the acceptance of *MAPF-1* section two magnetic quadrupole triplets *T1* and *T2* are used, Fig. 2. The triplets form at the *MAPF-1* input the bunches which are convergent in *xx'* and *yy'* cross sections of the beam phase space.

Particle losses along the drift between *RFQ* and *MAPF-1* sections do not exceed 0.01 %.

The needed power supply of *RFQ* section is  $P_1 \approx 105$  kW, and the average power is about  $\sim 2$  kW for the duty factor of 0.02.

#### 4. ALTERNATING-PHASE FOCUSING SECTIONS

As a rule after *RFQ* it is used accelerating structures based on cavities loaded by drift tubes [12]. Accelerating channel performances depend on the type of electromagnetic oscillations excited in the cavities and a method to ensure the transverse beam stability during ion acceleration. The structures based on *E*-mode oscillation were investigated sufficiently well (Alvarez structure). The length of accelerating periods for these structures equals  $\beta\lambda$ . Both ion accelerating and beam phasing (a longitudinal movement stability) are done by the *RF* field. To ensure the beam stability in transverse plane the alternating-sign magnetic focusing by the field of quadrupole geometry is used. For that the magnetic lenses (singlets) are located in the drift tubes.

The difficulties of manufacture of drift tubes in which electromagnetic lenses are located, necessity of their cooling, and number of lens power supply sources present problems if the accelerators with magnetic focusing channel are used for technological purposes.

Another approach to build a linac channel is based on alternating-phase focusing (*APF*). In this case the *RF* electrical field in gaps between drift tubes is used for phasing, accelerating and focusing of ions. To obtain the stable beam dynamics it is necessary to alter a sign, and vary a value of a synchronous particle phase  $\varphi_s$  in accelerating gaps. There are several ways to construct alternating-phase focusing channel, i.e. to separate the accelerating gaps into phasing ( $\varphi_s < 0$ ) and focusing ( $\varphi_s > 0$ ) periods by drift tube length variation. One way, so called a modified alternating phase focusing (*MAPF*), had been used to calculate the *MAPF-1* section, Fig. 2 [7].

In the accordance with the *MAPF* principle, to ensure the maximum stability of longitudinal beam movement, the synchronous particle phase in phasing periods has to be chosen  $\varphi_s \approx -90^\circ$ . However, the acceleration rate  $\Delta W/dz \sim \cos \varphi_s$  is low. Therefore to increase the mean acceleration rate it is necessary to take the minimum values of  $\varphi_s$  in focusing periods. Then the beam focusing hardness, which is proportional to  $\sin \varphi_s$ , is low. The results of numerical simulation show the optimal phase values in focusing gaps are in the range  $40^\circ \leq \varphi_s \leq 60^\circ$ .

If the numbers of phasing and focusing gaps in the focusing period are equal the resulting effect is the beam defocusing. Therefore the number of gaps with  $\varphi_s > 0$  must be higher than ones with  $\varphi_s < 0$ . Moreover with the growth of  $\beta$  for increasing of channel focusing hard-

ness it needs to increase the total number of accelerating gaps in the focusing period as  $\beta^{1/2}$  [7].

The calculated *MAPF-1* section with the input energy of 2 MeV and output one of 6.4 MeV has 3.24 m length and 37 accelerating periods of  $\beta\lambda/2$  length. The dependence of  $\varphi_s$  on the accelerating gap number is shown in Fig. 5. Phasing and focusing gaps form 5 focusing periods. The initial two gaps at the section input are to compress the divergent bunches in longitudinal direction after passing of the drift between *RFQ* and *MAPF-1*. The aperture radii of the drift tubes vary along the channel from 1.0 cm to 1.9 cm. The electrical field averaged over an accelerating gap is 130 kV/cm, and the maximum one on the drift tube surface is 300 kV/cm.

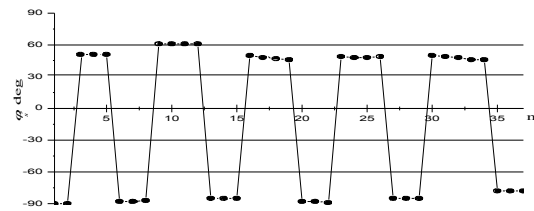


Fig.5. Dependence of a synchronous phase  $\varphi_s$  on a gap number  $n$  in the *MAPF-1* section

The integral equation method had been used for optimization of drift tube geometry, and calculation of the maximum electrical field on the tube surfaces and surface distribution of ohmic loss power density [14]. The particle losses in *MAPF-1* do not exceed of 0.01 %.

For an *APF*-channel the minimum length of a drift tube is determined by the value of accelerating electric field penetration into the tube but not the lens sizes, as for an Alvarez structure. Therefore the length of accelerating period for an *APF*-channel may be chosen shorter as  $\beta\lambda/2$ , i.e. the  $\pi$ -wave structure may be used. Therefore the number of accelerating periods increases for the same channel length and correspondingly the average acceleration rate.

To create the structure with the standing  $\pi$ -wave the *H*-mode cavities can be used. The transverse dimensions of *H*-cavities, loaded by drift tubes, decrease more than 4 times in comparison with *E*-cavities at the same oscillation frequency. For low  $\beta$  in *MAPF-1* and *MAPF-2* sections ( $0.0462 \leq \beta \leq 0.123$ ) the shunt impedance  $Z_{eff}$  of accelerating structures on the *H*-cavity base is high enough  $Z_{eff} \geq 50$  M $\Omega$ /m [16].

The calculated *MAPF-1* section has the *H*-cavity diameter of 40 cm and power consumption of  $P_2 \approx 0.85$  MW (average one is  $\sim 17$  kW).

The next *MAPF-2* section had been calculated analogically to *MAPF-1* one. The *MAPF-2* has the length of 3.78 m, and output deuteron energy of 14 MeV, and power consumption of  $P_3 \approx 1.45$  MW (average power  $\sim 29$  kW). The total number of accelerating periods is 32, which form 3 focusing periods. The aperture radii are varied from 2.0 cm to 2.9 cm. Particle losses in this section do not exceed 0.01 %.

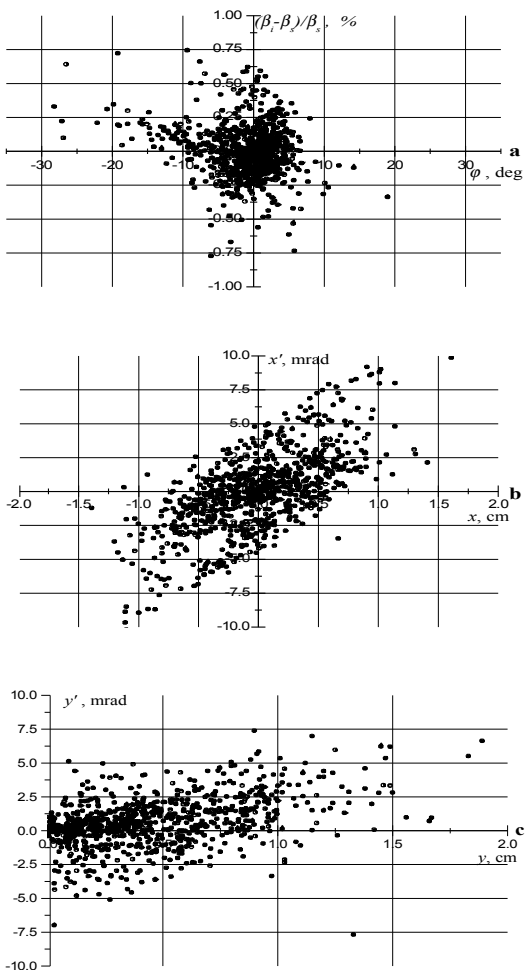


**Fig. 6.** Beam phase space plots at the linac output: a is longitudinal plane projection, b is  $xx'$  plane projection, c is  $yy'$  plane projection

The phase space performances of deuteron beam at the MAPF-2 output are given in Fig. 6. From Fig. 6 it follows the beam at the linac channel output is divergent in the transverse plane  $xy$  with transverse dimensions of  $1.8 \times 1.5$  cm, and convergent in the longitudinal direction.

The beam matching between the MAPF-1 and MAPF-2 had been done similarly as between RFQ and MAPF-1. Two magnetic quadrupole triplets  $T3$  and  $T4$ , Fig. 2, are matching beam parameters to the MAPF-2 acceptance. The longitudinal movement matching is reached due to the drift between MAPF-1 and MAPF-2. For that the last accelerating MAPF-1 periods are bunching ones for forming of convergent bunches in the longitudinal direction, Fig. 5.

The performed calculations had shown that the linac channel losses had varied inconsiderably if electric field deviations from the optimal value were in the limits from -1 % up to +4 %.

The effect of possible errors of manufacturing and assembling of RFQ, MAPF-1 and MAPF-2 construction elements on the beam dynamics had not been investigated in this work.

## REFERENCES

1. R.G. Benett, I.D. Christian, D.A. Petti et al. A System of  $^{99m}$ Tc Production Based on Distributed Electron Accelerators and Thermal Separation // *Nuclear Technology*. 1999, v. 126, p. 102-121.
2. Y. Jongen, P. Dhondt, L. Van Den Durpel et al. *Progress Report on ADONIS: the Proton-Driven Subcritical Reactor for Radioisotope Production*. Proceedings of the Second International Conference on Accelerator-Driven Transmutation Technologies and Applications, 1996, v. 1, p. 274-280, Kalmar, Sweden.
3. M.C. Lagunas-Solar et al. Cyclotron Production of NCA  $^{99m}$ Tc and  $^{99}$ Mo. An Alternating Non-Reactor Supply Source of Instant  $^{99m}$ Tc and  $^{99}$ Mo- $^{99m}$ Tc Generators // *J. Applied Radiation and Isotopes*. 1991, v. 42, №7, p. 643-657.
4. M. Sonck, S. Takacs, F. Szeleesenyi et al. *Excitation Functions of Deuteron Induced Nuclear Reactions on  $^{nat}$ Mo up to 21 MeV: Alternative Route for Production of  $^{94m,99m}$ Tc and  $^{99}$ Mo*. International Conference on Nuclear Data for Science and Technology, 1997, part II, p. 1637-1639, Trieste, Italy.
5. N.P. Dikiy, A.N. Dovbnya, V.L. Uvarov. *Development of New Electron Irradiation Based Technology for Technetium-99m Production*. Proceedings of the Sixth European Particle Accelerator Conference, 1998, p. 2389-2391, Stockholm, Sweden.
6. P.A. Demchenko et al. Application of Compact Linear Accelerators for Medicine // *Problems of Atomic Science and Technology, Series: Nuclear Physics Investigations*. 1997, №4,5(31,32), p. 168-170 (in Russian).
7. A.S. Beley, P.O. Demchenko, Ye.V. Gussev, M.G. Shulika. *An Alternating Phase Focusing Channel for Low Energy Proton Therapy*. Proceedings of the Seventh European Particle Accelerator Conference, 2000, p. 1477-1479, Vienna, Austria.
8. O.F. Nemetz, Yu.V. Gofman. *Handbook on Nuclear Physics*. Kiev: "Naukova dumka", 1975, 414 p. (R).
9. S. Takacs et al. New Cross-Sections and Intercomparision of Deuteron Monitor Reactions on Al, Ti, Fe, Ni and Cu // *Nucl. Instrum. and Methods B*. 2001, v. 174, p. 235.
10. I.M. Kapchinsky, V.A. Teplyakov. Linear Accelerator of Ions with Space Uniform Focusing // *Pribory i Tekhnika Experimenta*. 1970, №2, p. 19-21 (in Russian).
11. Z. Randa, K. Svoboda. Excitation Functions and Yields of the (d,p) Reactions on Natural Molybdenum for Deuteron Energies Less than 13 MeV // *J. Inorg. Nucl. Chem.* 1977, v. 39, p. 2121.
12. J.M. Lagnier. *Linac Architecture for High Power Proton Sources*. Proceedings of LINAC 2000 Conf., 2000, p. 1028-1032, Monterey, California, USA.
13. P.O. Demchenko, M.G. Shulika. Ion Beam Forming Dynamics in an Injector Taking into Account Plasma Boundary // *Problems of Atomic Science and Technology, Series: Nuclear Physics Investigations*. 2001, №3(38), p. 144-146.

14. P.O. Demchenko, M.G. Shulika. Optimization of Axially Symmetric Drift Tube Geometry // *Problems of Atomic Science and Technology, Series: Nucl. Phys. Investigations.* 2001, №5(39), p. 111-113.
15. V.A. Teplyakov, O. Vybore Parametrov NChU // *Problems of Atomic Science and Technology, Series: Nucl. Phys. Investigations.* 1992, №4(25), p. 27-29 (R).
16. *Linear Ion Accelerators*. Ed. by B.P. Murin. v. 2. M.: "Atomizdat", 1978, p. 20.